Est. 1984

ORIENTAL JOURNAL OF CHEMISTRY
An International Open Access, Peer Reviewed Research Journal

www.orientjchem.org

ISSN: 0970-020 X
CODEN: OJCHEG
2021, Vol. 37, No.(3):
Pg. 568-574

Synthesis and Properties of Ce^{3+} Doped Multi-functional TiO_2-SiO_2 Nanocomposite films

TRAN THI QUYNH NHU[1], TRAN TRONG AN[1], CAO XUAN THANG[1]*, NGUYEN VIET TUNG[2], NGUYEN THANH PHUONG[3] and LAI TRUNG TUNG[3]

[1]Advanced Institute for Science and Technology (AIST), Hanoi University of Science and Technology (HUST), No 01, Dai Co Viet Road, Hanoi, Vietnam.
[2]Institute of Science and Technology, Ministry of Public Security, No 100, Chien Thang Road, Hanoi, Vietnam.
[3]Research and Development Center of Kangaroo Groups, No 05, Dao Duy Anh Road, Hanoi, Vietnam.
*Corresponding author E-mail: thang.caoxuan@hust.edu.vn

http://dx.doi.org/10.13005/ojc/370307

(Received: April 01, 2021; Accepted: May 30, 2021)

ABSTRACT

The effect of Cerium on the properties of the multi-functional SiO_2-TiO_2:Ce^{3+} nanocomposite films are shown in this paper. The multi-functional SiO_2-TiO_2:Ce^{3+} nanocomposite film was synthesis by a sol-gel method and coated several layers on a glass substrate by a spin-coating technique. The bonding was indicated in the obtained film that Si-O-Si and Si-O-Ti bonding, which are characteristics that bonding in the SiO_2-TiO_2 matrix by the FT-IR spectrum. The TiO_2 crystal in the anatase phase and SiO_2 in the amorphous phase of the nanocomposite film was determined by X-ray Diffraction. When increased doping of Ce^{3+}, the prepared films have a high transmittance in the visible light (from 84.5 to 88.3%, 400 – 800 nm), the red-shifted of the absorbance edge in UV(A) region (from 355 to 390 nm), and the optical bandgap is narrowed. Particularly, the SiO_2-TiO_2:6%Ce^{3+} film has the transmittance by 88.3% in the visible light (400 – 800 nm), absorbance in the UV(A) light (390 nm), and performance the super-hydrophilic with/without thermal and UV(A) light. Thus, the multi-functional SiO_2-TiO_2:6%Ce^{3+} nanocomposite film could have a potential to use as the protective high transmittance film to avoid the UV-A light and exhibits a super-hydrophilic on the material surface such as glasses, photovoltaic devices, window panels.

Keywords: TiO_2/SiO_2 nanocomposite, TiO_2/SiO_2 thin films, Sol-gel, Ce^{3+} doped TiO_2/SiO_2.

INTRODUCTION

Materials used outdoors are often damaged by ultraviolet rays and extreme weather conditions or by mechanical collisions with other materials. In recent years, the development of nano-sized coatings that both ensure aesthetics and protect surfaces in extreme conditions is of particular concern. The most prominent is the thin film synthesized from TiO_2 material, which has been developed for a long time but is still current because of their application properties in the protective film field. Titanium dioxide

is a semiconductor oxide with a wide band gap, located in the ultraviolet region (3.0 – 3.2 eV)[1]. TiO_2 has attracted a lot of research scientists because it has interesting properties such as TiO_2 in Anatase phase with photocatalytic activity, self-cleaning ability, some studies show that TiO_2 materials are also capable of antibacterial[1-3]. However, Anatase phase has photocatalytic activity, under the effect of UV rays, can decompose organic components in artificial rocks, damaging the rock surface. In addition, Anatase phase is not stable to heat, when the heating temperature increases, TiO_2 materials have the ratio of Anatase and Rutile phases changes in the direction of increasing the Rutile phase ratio[4]. Moreover, TiO_2 has poor mechanical strength and ability to adhere to the surface of other materials.

As an alternative to TiO_2, silica-titania composite material, which is an oxide system consisting of silica (SiO_2) and titania (TiO_2), can be used. This material system has been the subject of research by many scientists because of the unique properties that come from the combination of these two separate oxides.

The silica-titania composite exhibits many desirable properties such as ultraviolet light absorption, TiO_2 self-cleaning, antimicrobial material, both the stability, mechanical strength of SiO_2, and incoming properties from chemical bonding between two materials[5-9]. In addition, silica and titania are both environmentally friendly, non-toxic, and low cost materials[2].

To enhance absorption and to improve some properties, materials can be doped with certain rare earth metals, transitional or nonmetallic. Cerium is a rare earth metal known for its many redox states. As an important doping material, cerium has advantages such as multiple electronic energy levels and valence states, which lead to different properties[10,11]. When doping cerium into the silica-titania composite material, there is a shift in the absorbed light from the ultraviolet to the visible light, enhancing the photocatalytic activity[11].

According to our knowledge, up to now, there has been no published study on the properties of Ce-doped TiO_2/SiO_2 nanocomposite thin film and orientation for application in the field of coating for outdoor use. In this study, we have proposed the successful synthesis of Ce-doped TiO_2/SiO_2 nanocomposite thin film by the sol gel method combined using the spin coating technique and their properties are discussed details.

EXPERIMENTAL

Materials

Tetraethyl orthosilicate (TEOS, 99% Sigma-Aldrich), Titanium tetra-n-butoxide (TBT, 98%, Sigma-Aldrich), Cerium (III) nitrate hexahydrate (Xilong Scientific) were used as starting materials. Isopropanol (IPA, 99.7%, Xilong Scientific), diethylene glycol (DEG, 99.7%, Xilong Scientific) were used as a solvent. The molar ratio of TEOS and TBT was optimized and fixed at 70:30.

Preparation

A series of TiO_2-SiO_2:xCe^{3+} nanocomposite films (x = 0 ÷ 0.08 mol) were prepared by the pechini-type sol-gel method and spin-coating technique. In the typical synthesis process, 7 mmol (1,55 mL) of TEOS was mixed with 25 mL IPA stirred for 10-15 minutes by a magnetic stirring hot plate at room temperature. Then HNO_3 and water were added into the solution, followed by stirring for 1 hour. Then, 3 mmol (1 mL) Titanium n-butoxide (TBT) was added into the solution which was further stirred for 1 hour. Thirdly, molar ratios of ($[Ce^{3+}]/([Ti^{4+}] + [Si^{4+}]$) with 2, 4, 6, and 8% of $Ce(NO_3)_3.6H_2O$ were alternatively added into the solution, then continuously stirred for 30 minutes. Finally, DEG (1 mL) was prepended as a cross linking agent and the stirring continued for 15 min to get a complete homogeneous solution. To prepared films form, they were spin-coated onto a glass substrate by a spin-coater machine, following two stages: 1500 rpm for 7s and 2500 rpm for 30s. Each of five nanocomposite layers on the glass substrate was dried at several times to evaporate solvents. After that, the five-layer films were annealed in the air at 100, 200, 300°C for 2 hours. The obtained nanocomposite films were employed to assess the further characterization.

Characterization

After obtaining the nanocomposite material, we carried out measurements to characterize and analyze the properties of the material. In detail, the Fourier-transform infrared spectroscopy (FT-IR, Spectrum Two, Perkin Elmer) was used to study the chemical bonding in the nanocomposite material.

The crystalline structure of nanocomposite films was studied by X-ray Diffraction (D8-ADVANCE, Bruker-Germany). The surface morphology of films was characterized by the high-resolution field emission scanning electron microscopy (FE-SEM,

JEOL JSM-7600F). The optical property of the films was investigated by using UV-Vis spectrophotometer (JASCO V-750). The wettability behavior was studied by the water contact angle measurement (WCA, C017).

RESULTS AND DISCUSSION

Figure 1. shows the XRD patterns of SiO_2-TiO_2:6% mol Ce^{3+} nanocomposite thin film on the glass substrate air-annealed at 100, 200 and 300°C for 2 h (a,b,c samples). The XRD patterns of (a,b) samples show that the films consist of SiO_2 and TiO_2 in the amorphous phase but at 300°C, the sample also existed anatase phase which is located at 2θ= 23° and TiO_2 crystals in the anatase crystal due to the characteristic peak at 2θ = 55.9°; 31.7°; 66.9° (PDF#84-1286). It is noteworthy that not all the peaks of the anatase phase and no peak of Ce crystal phase are observed in the XRD patterns. Such observed can be attributed to thickness of thin-film and the greater ionic radii of Ce^{3+} (0.107 nm) than Ti^{4+}, Si^{4+} (0.068, 0.040 nm, respectively). The difference in radii leads to difficulty for Ce^{3+} ions to replace Ti^{4+} or Si^{4+} ions in the SiO_2-TiO_2 matrix, hence, Ce^{3+} ions tend to bond with O_2- anion on the surface of TiO_2[12]. The trendy of bonding of Ce^{3+} with O_2- on its surface is a factor to influence the optical and wetting properties of the nanocomposite film that would be discussed in the next section.

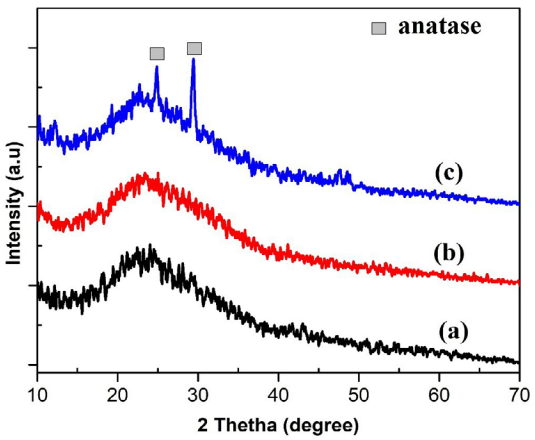

Fig. 1. X-Ray of Ce^{3+} doped TiO_2/SiO_2 with 6% mol concentration at different temperatures for 2 h (a:100°C; b: 200°C; c: 300°C)

The FT-IR spectra of SiO_2-TiO_2 and SiO_2-TiO_2:6%Ce^{3+} nano composite thin film (air-annealed at 300° for 2 h) shown in Fig. 2. The bands at 1070 cm^{-1} and 791 cm^{-1} can be assigned to the vibration of Si-O-Si bonding in SiO_2 and This trend indicated that vibration at 901 cm^{-1} may be resulted from the Ti-O-Si linkages Si-O-Ti bonding in TiO_2-SiO_2[13,14]. In this case, the content of Ce^{3+} is not sufficient to influence the vibration of bonding in the SiO_2-TiO_2 matrix.

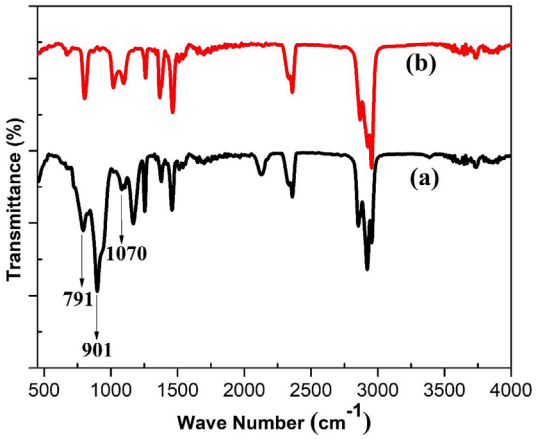

Fig. 2. FT-IR spectrum TiO_2/SiO_2 (a); TiO_2/SiO_2: 6% mol Ce^{3+} at 300°C for 2 hours

The morphology of SiO_2-TiO_2:x%Ce^{3+} nanocomposite films with a molar different ratio of Ce^{3+} (x = 0, 2, 4, 6, 8%) air-annealed at 300°C for 2 h is captured in the FE-SEM images (Fig. 3). As seen in FE-SEM images, the morphology of SiO_2-TiO_2 nanocomposite films change with respect to the amount of Ce^{3+} ions doped in the film. It is clearly seen, the composite film with x = 0% shows some cracks on its surface, however, these cracks disappear when increasing Ce^{3+} ratio to 2% (Fig.3b). In addition, the surface of SiO_2-TiO_2:x%Ce^{3+} composite films display the hole-like nanoparticles that distribute in the matrix with (x = 4%, 6%) (Fig.3. c, d) and the hole-like particles are distributed in the matrix having an average size of 50-100 nm. Further increasing the ratio of Ce^{3+} (x = 8%) in Fig. 3e, the cracks re-appear in the SiO_2-TiO_2:Ce^{3+} composite film surface. The appearance of particles on the nanocomposite film surface could be attributed to high enough concentration of Ce^{3+} doped in the film to induce phrase separation and form particles on the film surface.

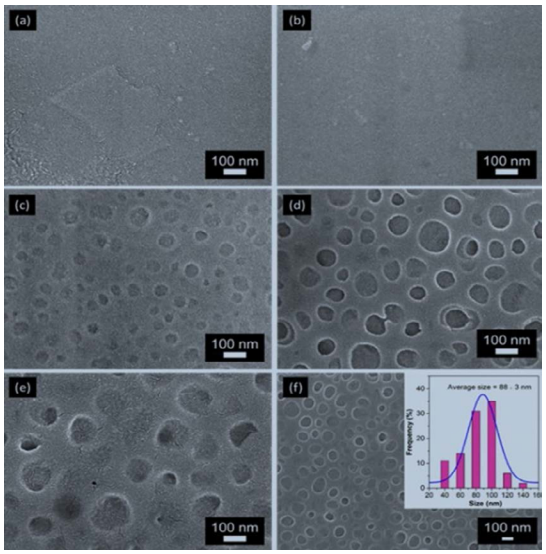

Fig. 3. FE-SEM images of Ce^{3+}-doped SiO_2-TiO_2 nanocomposite thin film at 300°C in the air for 2 h with a molar different ratio of Ce^{3+} (a) 0% (b) 2% (c) 4% (d) 6% (e) 8% (f) distribution of particles size of 6% Ce^{3+} sample

Figure 4 shows the UV-Vis transmittance spectrum of the obtained nanocomposite films. For the application of self-cleaning and protection, the film has to meet requirements of transmittance that greater than 85% in the visible region (400 – 800 nm), and absorbance in the UV-A region (300 – 400 nm)[8]. It is clear to observe that the concentration of Ce^{3+} ion-doped in the prepared film is a factor to effect to its optical properties. As shown in Fig. 4a, all of the wavelengths in the visible region (400 – 800 nm) can be transmitted through the film. By doping Ce^{3+}, the transmittance (T) of the SiO_2-TiO_2 film sample is raised from 84.5% to 88.3%. Because the intrinsic bandgap of SiO_2-TiO_2 composite is 3.0 – 3.4 eV[15]. In addition, the morphology of the Ce^{3+}-doped film surface shows that particles are distributed relatively with at least optical defects, due to low light scattering of the films, so then the transmittance of film increased. For all of those reasons, the visible light is easily transmitted in the nanocomposite film[15,16].

On the other hand, as can be seen in Fig. 4b, the absorbance is shifted towards longer wavelength from 300 - 420 nm to 355 to 390 nm, when the molar proportion of Ce^{3+} ions increases. The red-shifted of the absorbance can evidence for Ce^{3+} successfully doped in the SiO_2-TiO_2 matrix. However, with the Ce^{3+} concentration is 8%, the change is not significant in the UV-Vis spectrum, also in the FE-SEM image that could be the concentration of Ce^{3+} is saturated in the SiO_2-TiO_2 matrix. Consequently, the molar ratio of Ce^{3+} doped in the film is optimized at 6%.

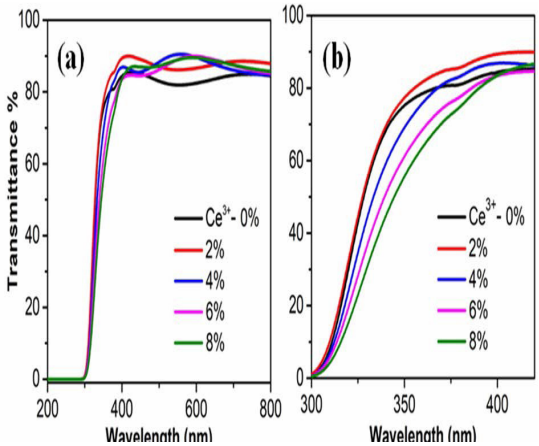

Fig. 4. UV-Vis transmittance spectrum of SiO_2-TiO_2:x%Ce^{3+} nanocomposite films with wavelength between (a) 200 – 800 nm (b) 300 – 420 nm

To investigate the effect of Ce^{3+} on the bandgap of the SiO_2-TiO_2 nanocomposite, the samples prepared and annealed at 300°C for 2 hours. Fig. 5 illustrates the UV-Vis Diffuse Reflection Spectrum (UV-Vis DRS) of the SiO_2-TiO_2:x%Ce^{3+}. In Fig. 5a, it can be seen that the absorption edge of the Ce^{3+}-doped in the samples is shifted towards the red-wavelengths when the Ce^{3+} concentration increase (from 390 to 530 nm). It is well known that the dopant can influence the structure of the host material. The configuration of Ce^{3+} is $[Xe]4f^15d^06s^0$ of which its f-orbital has unoccupied. When Ce^{3+} was doped in the SiO_2-TiO_2 matrix, the 4f electronic configuration of Ce which allows electron transition from 2p levels of oxygen (valance band – VB) to 4f levels of Cerium and 2p levels of Oxygen to 3d levels of Titanium (conduction band – CB)[17-21]. This leads to the generation of electron-hole pairs and the improvement of the visible light absorption, and visible light response.

According to the theory of P. Kulbelka and Munk[22] presented in 1931, the optical bandgap is calculated by applying the Kubelka-Munk function (1):

$$(F(R\infty)h\nu)^{1/\gamma} = B(h\nu - Eg) \quad (1)$$

Where $R\infty$ is the reflectance of an infinitely thick specimen, h is the Planck constant, ν is the photo's frequency, Eg is the bandgap energy, B is a constant. The γ factor depends on the nature of the

electron transition and is equal to ½ or 2 for the direct and indirect transition band gaps, respectively. It is known that SiO_2, TiO_2 are direct transition bandgap, therefore, Eg can be determined by plotting $(F(R\infty)h\nu)^2$ versus $h\nu$ the optical bandgap[23].

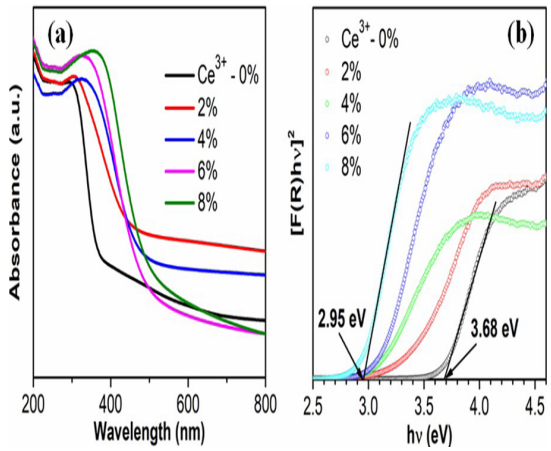

Fig. 5. UV-Vis Diffuse Reflection Spectrum of SiO_2-TiO_2:x% Ce^{3+} nanocomposite films (a) the UV-Vis absorbance spectrum (b) and the calculated band gap by Tauc plot

The optical bandgap of all samples is calculated and shown in Fig. 5b, for the SiO_2-TiO_2 nanocomposite sample, the optical bandgap is 3.68 eV, with absorbance wavelength is 337 nm, respectively. With an increase of molar ratio of Ce^{3+} doped in the SiO_2-TiO_2 matrix, the optical bandgap of obtained sample declines from 3.4 to 2.95 eV. When Ce^{3+} doped in the SiO_2-TiO_2 matrix, the 4f levels of Cerium are occupied, leads to new electric states in the bandgap of TiO_2, which were reported by Density-functional theory (DFT) simulation articles. According to DFT simulation for Ce^{3+} doped in the TiO_2, the 4f-Ce states are near conduction bands, they are shallow impurity states. This leads to the red-shifted of the absorption edge and the bandgap of the prepared nanocomposite material is narrowed. In addition, the shallow impurity levels are a factor to influenced the generation of photo-excited electron-hole pairs because they can trap the photo-excited electrons and holes[24]. Therefore, when Ce^{3+} is doped in the SiO_2-TiO_2 matrix, the optical properties of the SiO_2-TiO_2 nanocomposite is influenced.

The wettability of the nanocomposite films is investigated by the contact angle method (WCA). To further investigate the surfaces of the Cedoped SiO_2-TiO_2 nanocomposite films, the wettability behavior of the films was investigated by the water contact angle (WCA) method. Fig. 6 shows the water contact angle measurements for the non-coated sample and the sample coated with a layer of 6 mol% Ce-doped SiO_2-TiO_2 film after being exposed to UV (365 nm) for 30 minute. While the WCA of the noncoated sample did not change, the angle of the coated film changes from 43° to 11°. This result indicates that the surface of the sample has been transformed from a hydrophilic surface to a super-hydrophilic surface when coating with 6 mol% Ce-doped SiO_2-TiO_2 film. From the literatures, this transformation process can be explained by the creation of surface oxygen vacancies due to the appearance of TiO_2 nanocrystals in the coated film. In such system, the water molecules may travel into the oxygen vacancy sites, leading to the dissociative adsorption of the water molecules on the surfaces of coated film and the photoinduced reconstruction of surface hydroxyl groups. With the increase of adsorbed hydroxyl groups on the film surface, van der Waals forces and hydrogen bond interactions between water molecules and hydroxyl group will increase, leading to the super-hydrophilic properties of the composite film[25].

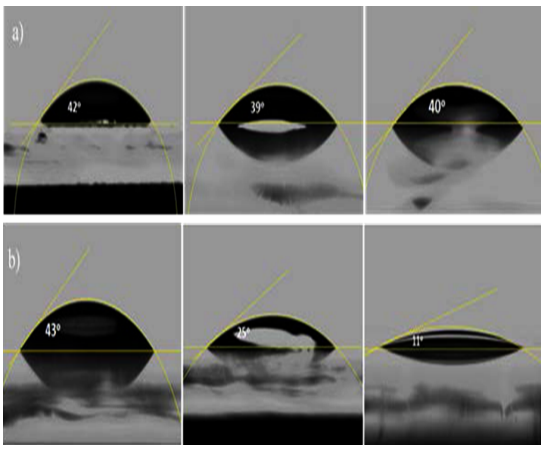

Fig. 6. The water contact angle of the SiO_2-TiO_2:6%Ce^{3+} nanocomposite film was exposed UV radiation 30 min (a: non-coated; b: coated by SiO_2-TiO_2:6%Ce^{3+})

CONCLUSION

In conclusion, the multi-functional SiO_2-TiO_2:x%mol Ce^{3+} nanocomposite film was successfully synthesized by sol-gel method. The results reported in this study illustrate that the

Ce^{3+} ion is a factor to influence the morphology, optical property, and the wetting of the obtained film. Particularly, the multi-functional SiO_2-TiO_2:6%mol Ce^{3+} nanocomposite film is a highly transmittance in the visible light (greater than 85%), absorbance in UV(A) light, and super-hydrophilic surface. For all of those results, the SiO_2-TiO_2:6%mol Ce^{3+} film is recommended to use as the protective film with some surfaces like glasses, photovoltaic devices.

ACKNOWLEDGEMENT

This research is funded by the Hanoi University of Science and Technology (HUST) under project number T2020-SAHEP-032. The author thankful to R&D center of Kangaroo groups for their kind support and motivation.

Conflict of interest

No conflict of interest.

REFERENCES

1. N. Mufti.; I.K.K. Laila.; Hartatiek, A. Fuad, *J. Phys. Conf. Ser.,* **2017**, *853*(1).
2. N. Rahimi.; R.A. Pax.; E.M.A. Gray.; *Prog. Solid State Chem.*, **2016**, *44*(3), 86-105.
3. Y. Hendrix.; A. Lazaro.; Q. Yu.; J. Brouwers.; *World J. Nano Sci. Eng.*, **2015**, *05*(04), 161-177.
4. Jaroenworaluck, A.; N. Pijarn.; N. Kosachan.; and R. Stevens, "Nanocomposite TiO_2-SiO_2 gel for UV-absorption," *Chem. Eng. J.,* 181–**2012**, *182*, 45–55.
5. Erdural, B.; U. Bolukbasi, and G. Karakas, "Photocatalytic antibacterial activity of TiO_2-SiO_2 thin films: The effect of composition on cell adhesion and antibacterial activity," *J. Photochem. Photobiol. A Chem.*, **2014**, *283*, 29–37.
6. Jesus, M. A. M. L. de.; J. T. da S. Neto.; G. Timò.; P. R. P. Paiva.; M. S. S. Dantas, and A. de M. Ferreira, "Superhydrophilic self-cleaning surfaces based on TiO_2 and TiO_2/SiO_2 composite films for photovoltaic module cover glass," *Appl. Adhes. Sci.*, **2015**, *3*, 1, 1–9.
7. Sun, S.; T. Deng.; H. Ding.; Y. Chen, and W. Chen, "Preparation of nano-TiO_2-coated SiO_2 microsphere composite material and evaluation of its self-cleaning property," *Nanomaterials.*, **2017**, *7*, 11.
8. Watanabe, F., "Composite resin.," Nihon Shika Ishikai Zasshi., **1971**, *24*(5), 483.
9. Zhang, S.; D. Sun.; Y. Fu, and H. Du, "Recent advances of superhard nanocomposite coatings: A review," Surf. *Coatings Technol.*, **2003**, *167*(2–3), 113–119.
10. Vázquez-Velázquez, A. R.; M. A. Velasco-Soto.; S. A. Pérez-García, and L. Licea-Jiménez, "Functionalization effect on polymer nanocomposite coatings based on TiO_2–SiO_2 nanoparticles with superhydrophilic properties," *Nanomaterials.*, **2018**, *8*, 6.
11. Zayat, M.; P. Garcia-Parejo, and D. Levy, "Preventing UV-light damage of light sensitive materials using a highly protective UV-absorbing coating," *Chem. Soc. Rev.*, **2007** , *36*(8), 1270–1281.
12. Maon, L., "Mohs' Scale of Hardness" *J. Chem. Inf. Model.*, **2013**, *53*(9), 1689–1699, 2013.
13. Latthe S.; Liu S.; Terashima C.; Nakata K.; Fujishima A Transparent, Adherent, and Photocatalytic SiO_2-TiO_2 Coatings on Polycarbonate for Self-Cleaning Applications. *Coatings.*, **2014**, *4*, 497–507. doi: 10.3390/coatings4030497.
14. Sun X.; Li C.; Ruan L.; Peng Z.; Zhang J.; Zhao J.; li Y Ce-doped SiO_2@TiO_2 nanocomposite as an effective visible light photocatalyst. *J Alloys Compd.*, **2014**, *585*, 800–804. doi: 10.1016/j.jallcom.2013.10.034
15. Latthe S.; Liu S.; Terashima C.; Nakata K.; Fujishima A Transparent, Adherent, and Photocatalytic SiO_2-TiO_2 Coatings on Polycarbonate for Self-Cleaning Applications. *Coatings.*, **2014**, *4*, 497–507. doi:10.3390/coatings4030497.
16. Guan K ., Relationship between photocatalytic activity, hydrophilicity and self-cleaning effect of TiO_2/SiO_2 films. *Surf Coatings Technol.*, **2005**, *191*, 155–160. doi: 10.1016/j.surfcoat.2004.02.022.
17. Jiang Y.; Jin Z.; Chen C.; Duan W.; Liu B.; Chen X.; Yang F.; Guo J Cerium-doped mesoporous-assembled SiO_2/P25 nanocomposites with innovative visible-light sensitivity for the photocatalytic degradation of organic dyes. *RSC Adv.*, **2017**, *7*, 12856–12870. doi: 10.1039/c7ra00191f.

18. Cao Y.; Zhao Z.; Yi J.; Ma C.; Zhou D.; Wang R.; Li C, Qiu J Luminescence properties of Sm3+-doped TiO_2 nanoparticles: Synthesis, characterization and mechanism. *J Alloys Compd.*, **2013**, *554*, 12–20. doi: 10.1016/j.jallcom.2012.11.149.
19. Devi LG, Kumar SG., Exploring the critical dependence of adsorption of various dyes on the degradation rate using Ln 3+ -TiO_2 surface under UV/solar light. *Appl Surf Sci.,* **2012**, *261*, 137–146. doi:10.1016/j.apsusc.2012.07.121.
20. Tsega M, Dejene FB Structural and optical properties of Ce-doped TiO_2 nanoparticles using the sol-gel process. ECS *J Solid State Sci Technol.*, **2016**, *5*, R17–R20.doi: 10.1149/2.0341602jss.
21. Yao Y.; Zhao N.; Feng JJ.; Yao MM.; Li F Photocatalytic activities of Ce or Co doped nanocrystalline TiO_2-SiO_2 composite films. *Ceram Int.*, **2013**, *39*, 4735–4738.doi: 10.1016/j.ceramint.2012.11.035.
22. Džimbeg-Malcic V.; Barbaric-Mikocevic Ž.; Itric K kubelka-munk theory in describing optical properties of paper (II). *Teh Vjesn* **2012**, *19*, 191–196.
23. Makuła P.; Pacia M.; Macyk W How To Correctly Determine the Band Gap Energy of Modified Semiconductor Photocatalysts Based on UV-Vis Spectra. *J Phys Chem Lett.,* **2018**, *9*, 6814– 6817. doi: 10.1021/acs.jpclett.8b02892.
24. Xie K.; Jia Q.; Wang Y.; Zhang W.; Xu J.; The electronic structure and optical properties of Anatase TiO_2 with rare earth metal dopants from first-principles calculations. *Materials (Basel).*, **2018**, *11*. doi: 10.3390/ma11020179.
25. Vidyadharan V.; Vasudevan P.; Karthika S.; Joseph C.; Unnikrishnan N V., Biju PR Structural, Optical and AC Electrical Properties of Ce3+-Doped TiO_2–SiO_2 Matrices. *J Electron Mater.*, **2015**, *44*, 2754–2761. doi: 10.1007/s11664-015-3724-6.